12WCEE 2000

ULTIMATE STRENGTH AND STRAIN OF CONCRETE STRUSTS IN IN-FILLED WALL PANELS OF FRAMED SHEARWALLS

Fumiya ESAKI[1]

SUMMARY

A new loading apparatus which can simulate the stress condition of cracked wall panels in framed shearwalls was proposed. By using the apparatus, the loading tests on the concrete strut specimens which were reinforced by either the orthogonal grid reinforcement in longitudinal and transverse directions or that in 45 deg direction were conducted. The shear strength of the wall panels observed by the tests agreed well with the shear strength of wall panels in framed shearwalls whose lateral load carrying capacity was dominated by the slip shear failure.

INTRODUCTION

The lateral load carrying capacity of monolithic R/C framed shearwalls (hereafter referred to as "shearwall") depends on the shear and axial strengths of their peripheral frame and the compressive capacity of the compressive struts formed in a cracked in-filled wall panel (hereafter referred to as "wall") [Tomii and Esaki, 1986 and 1987]. If the peripheral frame is sufficiently strong and properly reinforced, the compressive struts are crushed at an ultimate stage . This web crushing is the slip shear failure of the wall. The previous experimental studies on the compressive capacity of concrete struts in the wall have discussed the shear strength of the wall restrained only by wall reinforcements and subjected to constant external restraint forces [Miyahara, Kawakami and Maekawa, 1987, Veccio and Collins, 1986]. However, in order to clarify the lateral load carrying capacity of the shearwalls that failed in such shear, it is necessary to investigate the compressive capacity of concrete struts subjected to variable external restraint forces. As shown in Fig. 1, the wall in monolithic shearwalls is subjected to greater variable reaction forces from the peripheral frame which restrains the cracked wall against its dilatation due to shear cracking than from the wall reinforcements.

The aim of this study is to clarify the ultimate strength and strain of concrete struts in a wall reinforced by an orthogonal grid reinforcement whose directions are longitudinal and transverse and at a 45 deg.

2. LOADING TEST OF CONCRETE STRUTS

2.1 Loading Apparatus

The diagonal shear cracks occur in the wall if the shearwalls are subjected to lateral load. The cracked wall is subjected to variable reaction forces from the peripheral frame and the reinforcements since the cracked wall behaves as an anisotropic plate and consequently expands. The concrete struts formed between the cracks carry the lateral load. The cracks in the wall occur at a 45 deg since the wall is ordinarily reinforced by an orthogonal grid of reinforcement whose amount is same in both the longitudinal and transverse directions. If the condition is different from that mentioned above, the shear transfer is developed between the cracks. However, in this study it is assumed that the effect of the shear transfer on the ultimate strength is slight. It is estimated that the bond between the concrete and the reinforcement bars deteriorate at an ultimate stage. If there is no bond, the lateral load resisting mechanism of the shearwalls are as follows. The concrete bears the lateral load, and the reinforcements and the peripheral frame restrain the dilatation of the cracked

[1] *Faculty of Engineering, Dept. of Architecture, Kyushu Kyoritsu University, Japan. EmaI: ezaki@kyukyo-u.ac.jp*

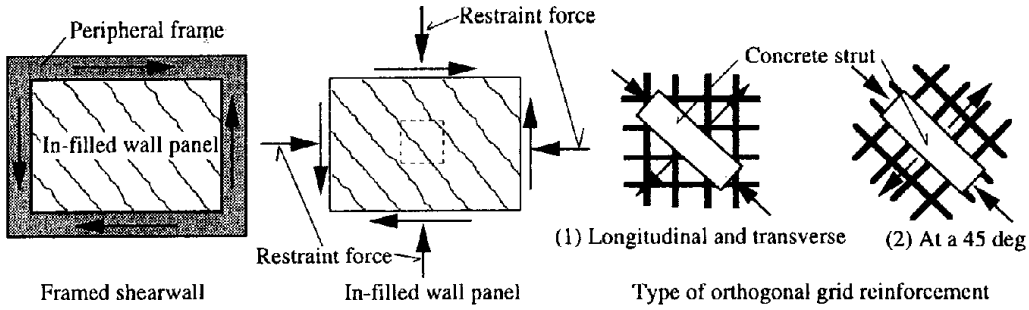

Fig. 1: Concrete struts formed in cracked wall of shearwalls and type of orthogonal grid reinforcement

wall. In this case the shear stress, τ, and the compressive stress, σ_c, are given by Eqs. 1 and 2 (see Figs. 1 and 2). If the peripheral frame does not fail in shear, the lateral load resisting capacity depends on the stress, σ_c in Eq. 2. In order to simulate the stress condition shown in Fig. 2, the loading apparatus shown in Fig. 3 was proposed. The four loading blocks are fastened to the anchorage plate for reinforcement, attaching to the ends of the specimens. As shown in Fig. 3, by compressing the four wedges inserted between the four blocks, the specimens can be subjected to compressive and tensile forces at the same time. The principal compressive stress, σ_c, the principal tensile stress, σ_t, and the external stress due to the restraining effect of the peripheral frame, σ_R, are given by Eqs. 3 and 4 as the function of the load, P,

$$\tau = {}_c\tau + {}_r\tau = p_s\sigma_s + \sigma_R \quad (1)$$

$$\sigma_c = {}_r\sigma_c + {}_c\sigma_c = 2(p_s\sigma_s + \sigma_R) \quad (2)$$

$$\sigma_c tb = \frac{P}{2} \quad (3)$$

$$(\sigma_t + \sigma_R)tl = \frac{P}{2}\tan\theta \quad (4)$$

$$\sigma_c = 2(\sigma_t + \sigma_R) \quad (5)$$

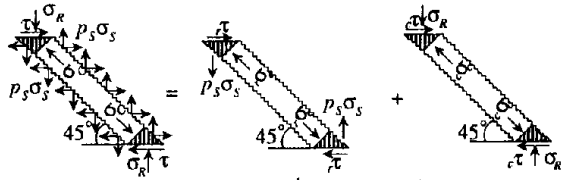

p_s = wall reinforcement ratio, σ_s = stress of reinforcement, σ_R = rastraint reaction stress, τ = shear stress, σ_c = compressive stress

Fig. 2: Stresses of struts

where b, l and t are the width, length and thickness of the specimens, respectively. The nominal dimensions of the specimens, l = 80cm and b = 20cm were decided by referring to the crack pattern in walls after an earthquake disaster or in lateral loading tests of shearwalls. In order to get the relation given by Eq. 2, the inclination of the wedges was decided as $\tan\theta = 2$.

2.2 Specimen

The nominal dimensions of the test specimens and the arrangement of the reinforcements are shown in Fig. 4. The properties of the test specimens are summarized in Table 1. The mechanical properties of reinforcement bars are summarized in Table 2.

The test series A were made to subject the specimens only a compressive force in the direction of the struts in order to investigate the behavior of the struts not subjected to a tensile force in the perpendicular direction to the struts. The test series B investigated the scatter of the strength and the strain at the ultimate stage under the same condition since the ultimate strength of the struts depended on the compressive strength of the concrete. The test series C investigated the effects of the restraining method against the dilatation of a cracked wall on the ultimate strength of struts. The test series D investigated the effect of the yield strength of reinforcements on the ultimate strength of the struts. The test series E investigated the effect of the arrangement direction of reinforcements on the ultimate strength of the struts.

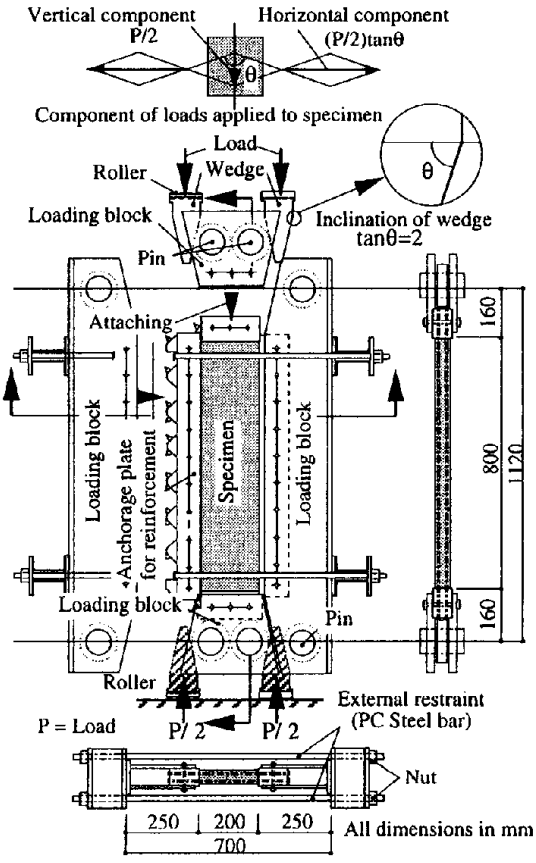

Fig. 3: Loading apparatus for struts

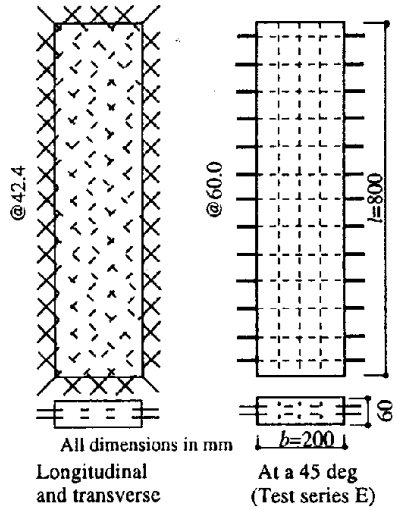

Fig. 4: Nominal dimensions of test specimens

2.3 Measurement system

As shown in Fig. 5, the compressive and tensile deformations between the bolts embedded at one point in the compressive direction and at three points in the tensile directions were measured by the high sensitive electric transducers. The strains of the reinforcement bars were measured by wire strain gauges pasted at the points shown in Fig. 5.

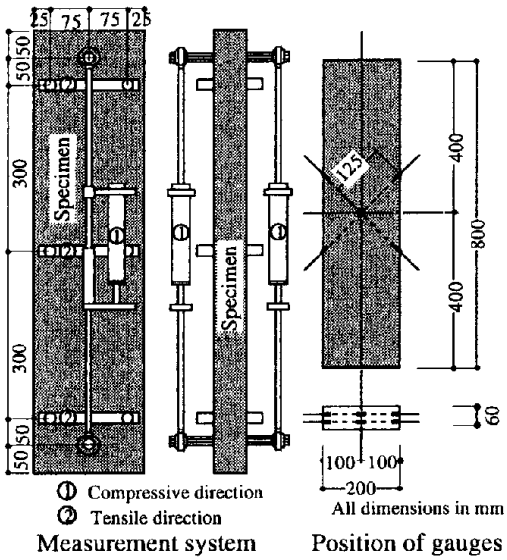

Fig. 5: Measurement system and position of gauges

Table 1: Properties of test specimens

Series	Specimen	Wall Reinforcements (p_s%)	$\sigma_B(E_c)$
A	2.36D	D6@42.4mm double(2.36)	24.7(26.2)
	0.59D	D6@84.8mm single(0.59)	
B	2.25D(1)	D6@42.4mm double(2.25)	25.8(23.7)
	2.25D(2)		
	2.25D(3)		
	1.12D(1)	D6@84.8mm double(1.12)	24.7(26.2)
	1.12D(2)		
	0.56D(1)	D6@84.8mm single(0.56)	25.8(23.7)
	0.56D(2)		
	0.56D(3)		
C	2.46DM	D6@42.4mm double(2.46)	29.4(26.5)
	1.22DM	D6@84.8mm double(1.22)	
	0.61DM	D6@84.8mm single(0.61)	
	2.46DH	D6@42.4mm double(2.46)	42.8(27.4)
	1.22DH	D6@84.8mm double(1.22)	
	0.61DH	D6@84.8mm single(0.61)	
D	1.56U(1)	U7.4@84.8mm double(1.56)	35.3(29.9)
	1.56U(2)		
	2.25DH(1)	D6@42.4mm double(2.25)	
	2.25DH(2)		
	1.05U(1)	U7.4@127.2mm double(1.05)	25.9(25.7)
	1.05U(2)		
	2.25DM	D6@42.4mm double(2.25)	
	0.78U(1)	U7.4@84.8mm single(0.78)	25.0(26.3)
	0.78U(2)		
	0.53U(1)	U7.4@127.2mm single(0.53)	25.8(25.2)
	0.53U(2)		
E	D1.67	D6@60mm double(1.67)	28.5(24.1)
	D1.11	D6@90mm double(1.11)	27.3(23.5)
	D0.83	D6@60mm single(0.83)	30.0(26.6)
	D0.56	D6@90mm single(0.56)	

p_s = wall reiforcement ratio, σ_B = compressive strength of concrete cylinder, E_c = Young's modulus of concrete

Table 2: Mechanical properties of reinforcements

Bar	a(cm²)	σ_y(MPa)	σ_u(MPa)	ε_l (%)
D6*1	0.300	407	538	22.9
D6*2	0.312	402	571	23.4
D6*3	0.286	474	597	18.0
U7.4	0.402	1435	1483	11.3

1) *1 = Series A, *2 = Series B, *3 = Series B, D and E
2) a = cross sectional area, σ_y = yield strength, σ_u = tensile strength, ε_l = elongation

2.4 Loading program

An incrementally increasing monotonic loading was adopted for this experiment. The nuts of the PC steel bars were loosened until the stress of the reinforcements reached the yield strength so that the external restraint force did not act on the specimens. When their stress nearly reached the yield strength, the nuts were attached to the loading blocks shown in Fig. 3 so that the force due to the PC bar's restraint reaction against the dilatation of the cracked wall acted on the specimens.

3. TEST RESULTS OF CONCRETE STRUTS

The relationships between the compressive stress, σ_c and the compressive strain, ε_c of the specimens in the test series

A are shown in Fig. 6. They agreed well with the stress-strain curves of the concrete cylinders. This fact means that the stress-strain relationships of the struts subjected to the compressive load only in the direction of the struts are approximately same as those of the concrete cylinders since the compressive stress at the crushing, σ_{cu}, agreed well with the compressive strength of the concrete cylinders, σ_B. The compressive stress and strain at the crushing, σ_{cu} and ε_{cu} in the test series B are summarized in Table 3. The crushing of the struts occurred in the specimens 2.25D series before and in the specimens 0.56D series after the external restraint force acted, respectively. The standard deviation and the coefficient of variation indicated as the degree of the scatter of the stress and strain at the crushing agreed well with those of the concrete cylinders (standard deviation = 0.534MPa, $0.15(10^{-3})$ and coefficient of variation = 0.02, 0.07).

The examples of the relationships between σ_c and ε_c, and between σ_c and tensile strains in the perpendicular to the direction of the struts, ε_t, for the specimens reinforced by the orthogonal grid reinforcements of the garde 400MPa and 1400MPa in the longitudinal and transverse directions are shown in Fig. 7. In this figure the cracking patterns at the ultimate stage are also shown. In the early loading stage the tensile cracking occurred scarcely and consequently the tensile strain was small. The lower the wall reinforcement ratio was, the stronger this tendency was. This fact is due to that the stress transfer to the concrete due to the bond stress of the reinforcements was less in the specimens reinforced lightly than in those reinforced heavily. As shown in Fig. 8, the strain of the reinforcement at the center of the strut, $_s\varepsilon_t$, was nearly zero, but ones at the ends increased as the compressive stress of the strut, σ_c increased at the early loading stage. However, the strain at the center as well as ones at the ends increased after the tensile cracking occurred. This fact means that the tensile force was transferred to the concrete by the bond stress of the reinforcements. The compressive stress at the crushing was lower than the compressive strength of the concrete cylinders in the specimens with each

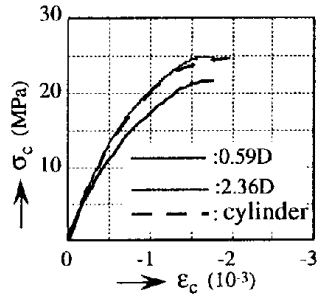

Fig. 6: Stress-strain curves in test series A

Table 3: Summary of results in test series B

Specimen	σ_{cu}(MPa)		$\varepsilon_{cu}(10^{-3})$	
2.25D(1)	19.1	X=18.5	2.40	X=2.17
2.25D(2)	18.2	Y=0.399	1.94	Y=0.19
2.25D(3)	18.3	Z=0.02	2.17	Z=0.09
0.56D(1)	18.3	X=19.5	2.02	X=1.89
0.56D(2)	19.7	Y=0.865	1.81	Y=0.09
0.56D(3)	20.4	Z=0.04	1.83	Z=0.05

σ_{cu} = compressive stress at the crushing of struts, ε_{cu} = compressive strain at the crushing, X = mean value, Y = stndard deviation, Z = coefficient of variation

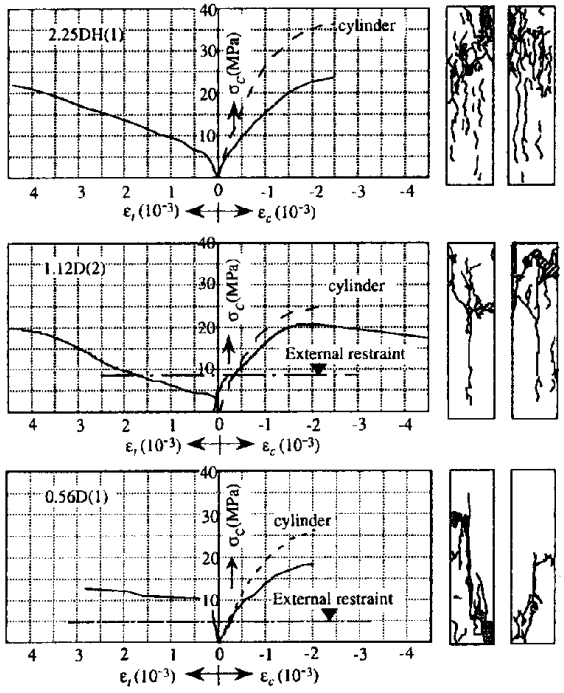

Fig. 7a: Stress-strain curves and crack patterns in specimens with reinforcements of grade 400MPa in longitudinal and transverse directions

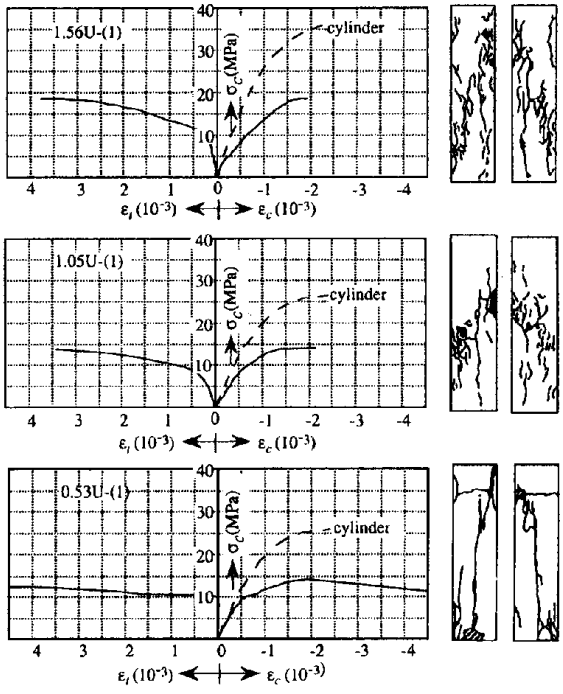

Fig. 7b: Stress-strain curves and crack patterns in specimens with reinforcements of grade 1400MPa in longitudinal and transverse directions

grade reinforcements. This tendency was stronger in the specimens with the grade 1400MPa than in those with the grade 400MPa. As indicated in the reference [Veccio and Collins, 1986], the fact was due to that the tensile force acted on the struts in the perpendicular direction to the principal compressive one and also that the effect of the additional axial force due to the compulsive flexure of the reinforcements shown in Fig. 9 was larger in the specimens with the high grade reinforcements than in those with the low grade ones .

The examples of the relationships between σ_c and ε_c and between σ_c and ε_t for the specimens in the test series E are shown in Fig. 10. The force acting on the reinforcement was excluded from the compressive force to calculate the compressive stress of the strut, σ_c. The number of cracks was fewer and the cracking load was higher in the test series E than in the test specimens with the orthogonal grid reinforcement in longitudinal and transverse directions. Also, the compressive stress at the crushing agreed well with the compressive strength of the concrete cylinders. This fact is due to that the tensile force was less transferred to the concrete by the bond stress of the reinforcements since the development length of the reinforcements was shorter in this case than in the case of the reinforcements in longitudinal and transverse directions, and that the additional force due to the compulsive flexure of the reinforcement did no act on the concrete strut. The compressive stress at the crushing of the struts, σ_{cu}, the strain at the crushing, ε_{cu}, and the effective coefficient for the compressive strength of the concrete struts, ν, are summarized in Table 4. The effective coefficient, ν, were defined as the ratio of σ_{cu} to $\sqrt{\sigma_B}$, where σ_B was the compressive strength of the concrete cylinder. The relationships between ν and reinforcement ratio, p_s, and between ν and the tensile strain in the perpendicular direction to the compressive one, ε_{tu}, at the crushing are shown in Fig. 11, respectively. According to this figure, the value of ν was approximately constant since it was not affected by the existence of the external restraint action and also by the experimental

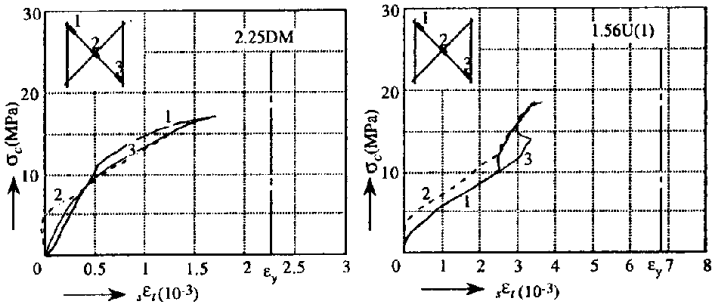

Fig. 8: Examples of compressive stress of struts, σ_c, - tensile strain of reinforcements, $_s\varepsilon_t$, curves

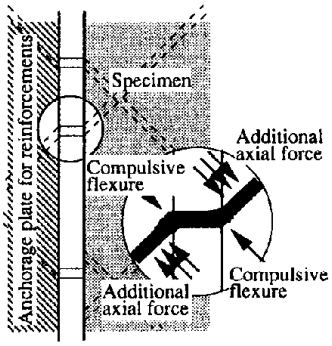

Fig. 9: Additional axial force due to compulsive flexure of reinforcements

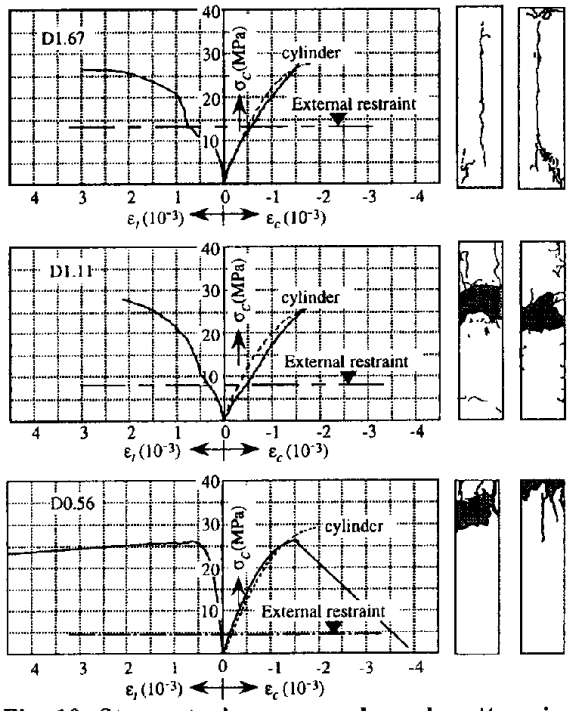

Fig. 10: Stress-strain curve and crack pattern in specimens with reinforcements of grade 400MPa in 45 deg direction

Table 4: Summary of results in tests of struts

Series	Specimen	σ_{cu} (MPa)	ε_{cu} (%)	$\frac{\sigma_{cu}}{\sqrt{\sigma_B}}$	Series	Specimen	σ_{cu} (MPa)	ε_{cu} (%)	$\frac{\sigma_{cu}}{\sqrt{\sigma_B}}$
B	2.25D(1)	19.1	0.240	3.76		1.56U(1)	18.1	0.192	3.05
	2.25D(2)	18.2	0.194	3.59		1.56U(2)	15.5	0.168	2.61
	2.25D(3)	18.3	0.217	3.61		2.25DH(1)	22.7	0.249	3.83
	1.12D(1)	20.2	0.188	4.06		2.25DH(2)	21.9	0.217	3.68
	1.12D(2)	19.3	0.400	3.88		1.05U(1)	13.8	0.214	2.72
	0.56D(1)	18.3	0.202	3.61	D	1.05U(2)	14.0	0.179	2.76
	0.56D(2)	19.7	0.181	3.88		2.25DM	16.8	0.238	3.29
	0.56D(3)	20.4	0.183	4.02		0.78U(1)	15.0	0.224	3.00
C	2.46DM	17.3	0.192	3.20		0.78U(2)	15.1	0.148	3.02
	1.22DM	16.4	0.170	3.02		0.53U(1)	13.9	0.193	2.74
	0.61DM	21.7	0.173	3.99		0.53U(2)	16.7	0.170	3.28
	2.46DH	22.1	0.169	3.37	E	D1.67	26.6	0.151	4.98
	1.22DH	28.4	0.174	4.34		D1.11	27.6	0.221	5.28
	0.61DH	24.5	0.122	3.74		D0.83	27.1	0.185	4.94
						D0.56	25.9	0.153	4.73

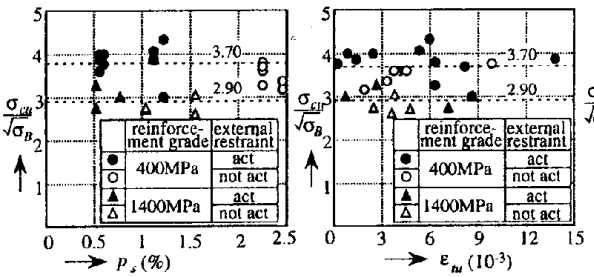

Fig. 11: Relationships between ν and p_s, and between ν and ε_{tu} in specimens with reinforcements in longitudinal and transverse directions, respectively

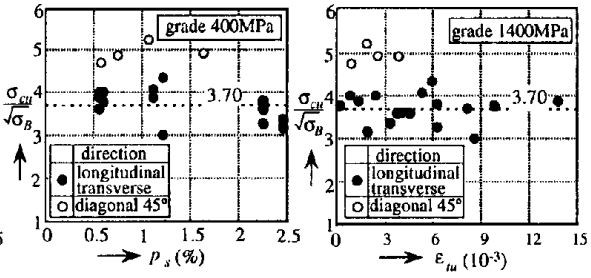

Fig. 12: Relationships between ν and p_s, and between ν and ε_{tu} in specimens with reinforcements of grade 400MPa, respectively

variable factors, p_s and ε_{tu}, if the specimens were reinforced by the same grade bars. However, the effective coefficients in the specimens reinforced by the bars of the grade 1400MPa were smaller than those in the specimens reinforced by the bars of the grade 400MPa. The mean values of the compressive strength of the struts, σ_{cu}, for the test series of the grade 400MPa bars and for those of the grade 1400MPa bars are given by Eqs. 6 and 7. Using Eqs. 1 and 2, the ultimate shear strengths of the walls are given by Eqs. 8 and 9. The effective coefficients for the specimens reinforced by the orthogonal grids of the grade 400MPa bars in longitudinal and transverse directions and in 45 deg direction are shown in Fig. 12. The mean values of ν for the specimens with the reinforcements in 45 deg direction was larger than those for specimens with the reinforcements in longitudinal and transverse directions.

$$\sigma_{cu} = 3.70\sqrt{\sigma_B} \quad \text{(MPa) for walls with reinforcements of grade 400MPa} \tag{6}$$

$$\sigma_{cu} = 2.90\sqrt{\sigma_B} \quad \text{(MPa) for walls with reinforcements of grade 1400MPa} \tag{7}$$

$$\tau_u = 1.85\sqrt{\sigma_B} \quad \text{(MPa) for walls with reinforcements of grade 400MPa} \tag{8}$$

$$\tau_u = 1.45\sqrt{\sigma_B} \quad \text{(MPa) for walls with reinforcements of grade 1400MPa} \tag{9}$$

4. LATERAL LOADING TESTS OF SHEARWALLS

In order to investigate the relationship between the shear strength of the wall obtained by the loading tests of concrete struts and that obtained by the lateral loading tests of shearwalls, the lateral loading tests on the shearwalls, whose peripheral columns were reinforced by the two types of H-shaped steel (see Fig. 13), were conducted. The specimens were subjected to the reversed cyclic lateral load under a variable axial load by using the loading apparatus shown in Fig. 14. The two types of loading velocity, 0.01cm/sec for the static loading (S - series) and 1cm/sec for dynamic loading (D - series), were adopted. The peripheral columns and wall were reinforced by the reinforcement bars and steel of the grade 400MPa. The load - displacement hysteresis envelope curves of all specimens are shown in Fig. 15. The failure mode was the slip shear of the wall in all specimens. The test results are summarized in Table 5. The shear strength of the shearwalls, $_{ex}\tau_u$, obtained by Eq. 10 agreed well with the results obtained by the loading tests of the struts. In Eq. 10, κ_w is the shape factor for the shear stress at the center of the wall and is obtained by the I-shaped beam theory [Tomii, 1957].

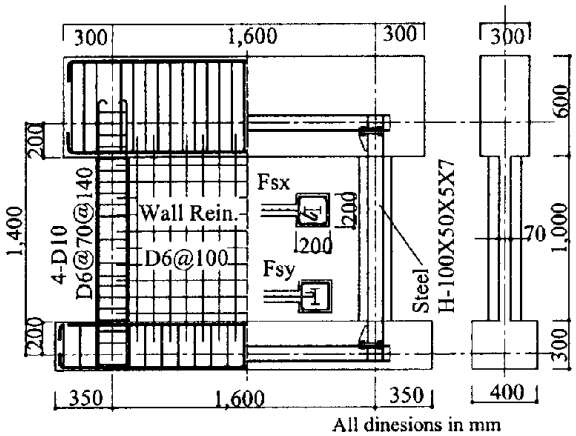

Fig. 13: Nominal dimensions of shearwall specimens

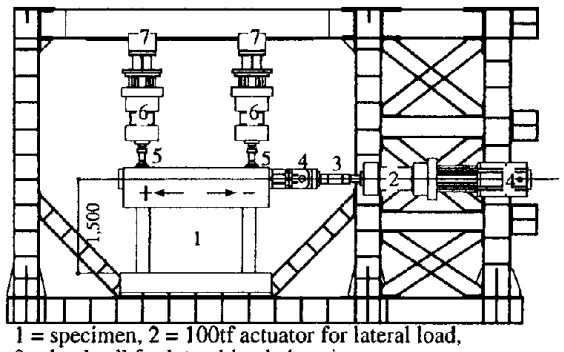

1 = specimen, 2 = 100tf actuator for lateral load,
3 = load cell for lateral load, 4 = pin,
5 = load cell for vertical load,
6 = 50tf actuator for vertical load, 7 = roller

Fig. 14: Loading apparatus for shearwalls

It was indicated in the reference [Tomii and Hiraishi, 1979] that the shape factor changed and became larger after the cracking than at an elastic stage. However, it is expected that the redistribution of the shear stress occurs in some zones. In this investigation, the shape factor at an elastic stage was employed because of the reason mentioned above.

$$ {}_{ex}\tau_u = K_w \frac{{}_{ex}Q_u}{tl} \qquad (10) $$

where,

${}_{ex}Q_u$ = experimental value of lateral load carrying capacity

t = thickness of wall

l = distance between center of edge columns

Table 5: Summary of results in tests of shearwalls

Specimen	σ_B (MPa)	${}_{ex}Q_u$ (kN)		$\frac{K_w \cdot {}_{ex}Q_u}{tl\sqrt{\sigma_B}}$	
		+	-	+	-
FsxW7-S	18.7	656	647	1.58	1.56
FsxW7-D		701	729	1.71	1.76
FsyW7-S		650	621	1.57	1.50
FsyW7-D		722	673	1.74	1.63

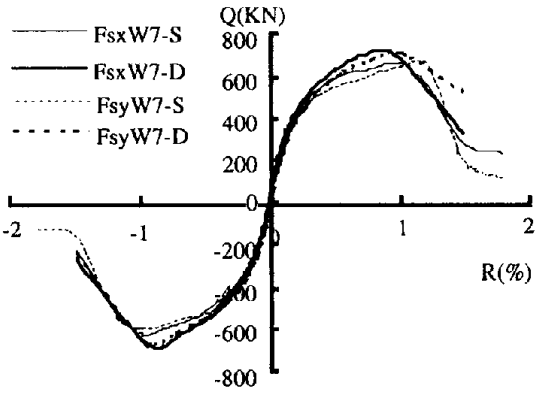

Fig. 15: Lateral load, Q - Story drift angle, R envelope curves

5. ULTIMATE SHEAR STRENGTH OF WALL PANEL OF SHEARWALLS

In order to investigate the ultimate shear strength of a wall moreover, the experimental data [Esaki, Tomii and Mitsuyama, 1988] for the isolated one-story shearwalls simulating multistory ones by making their edge beams rigid were employed . The relationships between the ratio of ${}_{ex}\tau_u$ to $\sqrt{\sigma_B}$, $\mu = {}_{ex}\tau_u / \sqrt{\sigma_B}$ (hereafter referred to as the shear strength coefficient of the wall) and the experimental variables related with the restraint to the cracked wall are shown in Figs. 16 and 17. The experimental values of the shear stress of the wall at the shear failure, ${}_{ex}\tau_u$, are obtained by Eq. 10.

According to Figs. 16 and 17, the shear strength coefficient of the wall, μ, did not correlate with the experimental variables related with the restraint to the dilatation of the cracked wall. Also, the effect of the shear span ratio M/Ql on the shear strength of the wall was scarcely as shown in Fig. 17. Assuming that the shear strength coefficient of the wall

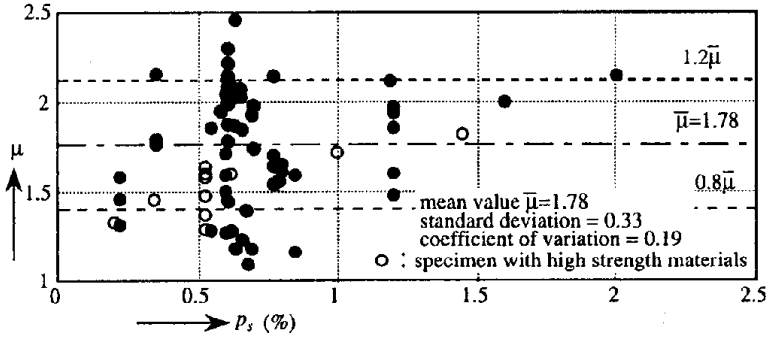

Fig. 16: Relation between shear strength coefficient of wall, μ and wall reinforcement ratio, p_s

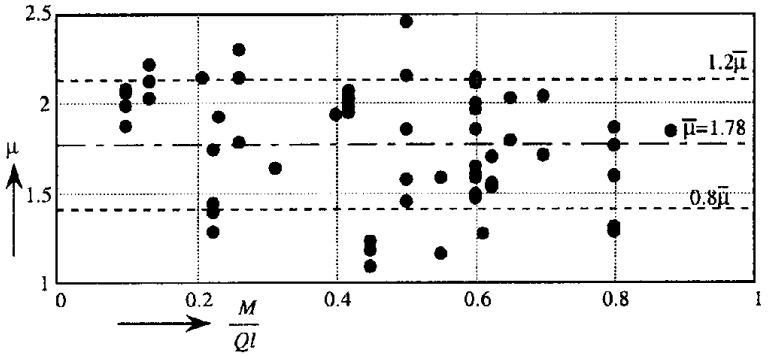

Fig. 17: Relation between shear strength coefficient of wall, μ and shear span ratio, M/Ql

is approximately constant, the shear strength of the wall, ${}_{ex}\tau_u$, is given by Eq. 11. Eq. 11 is close to Eq. 8. This fact means that the lateral load carrying capacity of the shearwalls which were dominated by the slip failure can be estimated by the experimental results mentioned in the former paragraph. The values obtained by Eq. 11 are smaller than those by Eq. 8. This is due to the effect of the cyclic loading since Eq. 11 was derived by the cyclic loading tests, while Eq. 8 was derived by the monotonic loading tests. The experimental data of the specimens with the high strength materials [Kanemoto, Matsumoto and Kabeyasawa, 1990, Saitoh, Kuramoto and Minami, 1990 and Yanagisawa, et. al, 1992] were also shown in Fig. 16. Those shear strength coefficients tended to be smaller than those with the ordinary strength materials as well as the experimental results in this paper.

$$ {}_{ex}\tau_u = 1.78\sqrt{\sigma_B} \tag{11}$$

6. CONCLUSIONS

In order to simulate the diagonal compressive struts formed in the cracked wall, a new loading apparatus was proposed. The experiments of the struts were conducted by using this apparatus, and the following are concluded.

1. The degree of the scatter for the compressive stress and strain at the crushing of the struts is approximately same as that for the compressive strength and strain at the peak stress of the concrete cylinder.
2. The effective coefficient of the compressive strength for the concrete struts, ν, which is the ratio of the compressive stress at the crushing to the square root of compressive strength of the concrete cylinder, is approximately constant.
3. The coefficient, ν, for the specimens with the reinforcements of the grade 1400MPa is smaller than that with the reinforcements of the grade 400MPa.
4. The ultimate shear strength of the wall in the shearwalls failed in slip shear agreed well with the strength obtained by the experiments of the struts.

7. ACKNOWLEDGMENTS

This experiments were conducted under a Grant from Kyushu Kyoritsu University (KKU). Many students at KKU assisted the experiments. Messrs. Tetsuo Kuriyama and Osamu Aoki who are the technicians at KKU assisted the manufactured of the test setup and specimens. The high strength reinforcement bars which were arranged in the specimens offered by NETSUREN CO.LTD.

The author thanks all the people and company described above for their contribution to this study.

8. REFERENCES

Esaki, F., Tomii, M. and Mitsuyama, H. (1983), " Effect of Vertical Load on Lateral Shear Capacity of Multistory Framed Shear Wall Failed in Shear," *Reports of Kyushu Chapter of AIJ*, No. 30, pp.321-324, (in Japanese).

Kanemoto, K., Matsumoto, K. and Kabeyasawa, T. (1990), " Hysteretic Behavior of High Strength Reinforced Concrete Shear Walls in Flexural Failure, part 1 - 2," *Summaries of Technical Papers of Annual Meeting of AIJ*, pp.607-610, (in Japanese).

Miyahara, N., Kawakami, Y. and Maekawa, K. (1987), " Nonlinear Behavior of Cracked Reinforced Concrete Plate Element Under Uniaxial Compression ," *Transactions of JSCE*, pp.249-258, (in Japanese).

Saitoh, F., Kuramoto, H. and Minami, K. (1990), " Shear Behavior of Walls Using High Strength Concrete," *Summaries of Technical Papers of Annual Meeting of AIJ*, pp.605-606, (in Japanese).

Tomii, M. (1957), " Studies on Shearing Resistance of Reinforced Concrete Plates," *Report of the Institute of Industrial Science University of Tokyo*, Vol. 6, No. 3, pp.1-45, (in Japanese).

Tomii, M. and Hiraishi, H. (1979), " Elastic Analysis of Framed Shear Walls by Assuming Their Infilled Panel Walls to be 45-Degree Orthotropic Plates, part 2 Numerical Examples," *Transactions of AIJ*, No. 284, pp.51-61.

Tomii, M. and Esaki, F. (1986), " Expression for Calculating Lateral Shear Capacity of One-Bay One-Story Reinforced Framed Shear Walls Dominated Slip Failure of Their In-filled Wall Panel," *Journal of Structural and Construction Engineering (Transactions of AIJ)*, No. 366, pp.142-154.

Tomii, M. and Esaki, F. (1987), " Lateral Shear capacity of One-bay One-story Reinforced Concrete Framed Shear Walls Whose Edge Columns or Beams Failed in Shear," *Journal of Structural and Construction Engineering (Transactions of AIJ)*, No. 376, pp.81-91.

Veccio, F. and Collins, M. F. (1986), " The Modified Compression Field Theory for Reinforced Concrete Elements subjected to Shear," *ACI Journal, Mar/Ap*, pp.219-231.

Yanagisawa, N., et. al (1992), " Study on High Strength Reinforced Concrete Shear Walls, part 1 - 3," *Summaries of Technical Papers of Annual Meeting of AIJ*, pp.347-352, (in Japanese).